Chemistry and Physics of Lipids 198 (2016) 21–27

Contents lists available at ScienceDirect

Chemistry and Physics of Lipids

journal homepage: www.elsevier.com/locate/chemphyslip

Effect of local anesthetics on the organization and dynamics in membranes of varying phase: A fluorescence approach

Sandeep Shrivastava[1], Diya Dutta[1], Amitabha Chattopadhyay*

CSIR-Centre for Cellular and Molecular Biology, Uppal Road, Hyderabad 500 007, India

ARTICLE INFO

Article history:
Received 5 April 2016
Accepted 29 April 2016
Available online 3 May 2016

Keywords:
DPH
TMA-DPH
Phenylethanol
Membrane phase
Local anesthetics

ABSTRACT

The molecular mechanism underlying the action of local anesthetics remains elusive. Phenylethanol (PEtOH) is an ingredient of essential oils with a rose-like odor and has been used as a local anesthetic. In this work, we explored the effect of PEtOH on organization and dynamics in membranes representing various biologically relevant phases using differentially localized fluorescent membrane probes, DPH and TMA-DPH. We show here that PEtOH induces disorder in membranes of all phases (gel/fluid/liquid-ordered). However, the extent of membrane disorder varies in a phase-specific manner. Maximum membrane disordering was observed in gel phase, followed by liquid-ordered membranes. The disordering was minimal in fluid phase membranes. Interestingly, our results show that the disordering effect of PEtOH in gel phase is sufficiently large to induce phase change at higher PEtOH concentrations. Our results are relevant in the context of natural membranes and could be useful in understanding the role of anesthetics in membrane protein function.

1. Introduction

Local anesthetics are a class of compounds that suppress sensation in a limited area of application in the body by reversibly blocking the action potential responsible for neuronal transmission, thereby relieving pain. The molecular mechanism underlying the action of local anesthetics is not completely understood. The question of whether anesthesia results from an indirect anesthetic-lipid environment effect (Arias, 1999) or a specific anesthetic-protein interaction (Rehberg et al., 1995) remains elusive.

Phenylethanol (PEtOH) (see Fig. 1a) is an ingredient of essential oils with a rose-like odor which has been used as a local anesthetic (Anbazhagan et al., 2010; Gray et al., 2013). PEtOH is one of the most important contributors of aroma in several fresh fruits such as tomato (Tieman et al., 2006). PEtOH has been reported to alter membrane order by altering lipid packing (Anbazhagan et al., 2010; Jordi et al., 1990; Killian et al., 1992). In addition, PEtOH has been shown to induce translocation of the mitochondrial precursor protein apocytochrome *c* (Jordi et al., 1990), and influence oligomerization of membrane proteins by altering helix-helix interaction (Anbazhagan et al., 2010).

In this paper, we have utilized two depth-dependent fluorescent membrane probes DPH and TMA-DPH (see Fig. 1b) to comprehensively explore the interaction between PEtOH and membranes of varying phases. Since the membrane bilayer represents a two-dimensional anisotropic fluid, any possible change in membrane order may not be uniform and restricted to a unique location in the membrane. It is therefore important to monitor the change in membrane order at more than one location. We have previously shown that stress such as heat shock can induce anisotropic changes in membrane order, *i.e.*, the change in membrane order could vary when monitored in different regions of the membrane (Revathi et al., 1994). In addition, such depth-dependent modulation of membrane order induced by alcohols (Kitagawa and Hirata, 1992) has been previously reported. DPH is a rod-like molecule and partitions into the interior of the bilayer. TMA-DPH is a derivative of DPH with a cationic moiety attached to the *para* position of one of the phenyl rings (Prendergast et al., 1981). While DPH is known to be located in the hydrophobic region of the membrane, the amphipathic TMA-DPH is localized in the shallower region of the bilayer with its positive charge anchored at the membrane interface. Its DPH moiety is located at ~11 Å from the center of the bilayer and provides information from the membrane interface (Kaiser and London, 1998). In contrast to this,

Abbreviations: DMPC, 1,2-dimyristoyl-*sn*-glycero-3-phosphocholine; DPH, 1,6-diphenyl-1,3,5-hexatriene; DPPC, 1,2-dipalmitoyl-*sn*-glycero-3-phosphocholine; LUV, large unilamellar vesicle; PEtOH, phenylethanol; POPC, 1-palmitoyl-2-oleoyl-*sn*-glycero-3-phosphocholine; TMA-DPH, 1-[4-(trimethylammonio)phenyl]-6-phenyl-1,3,5-hexatriene.

* Corresponding author.
E-mail address: amit@ccmb.res.in (A. Chattopadhyay).

[1] These authors contributed equally to this work.

http://dx.doi.org/10.1016/j.chemphyslip.2016.04.009
0009-3084/

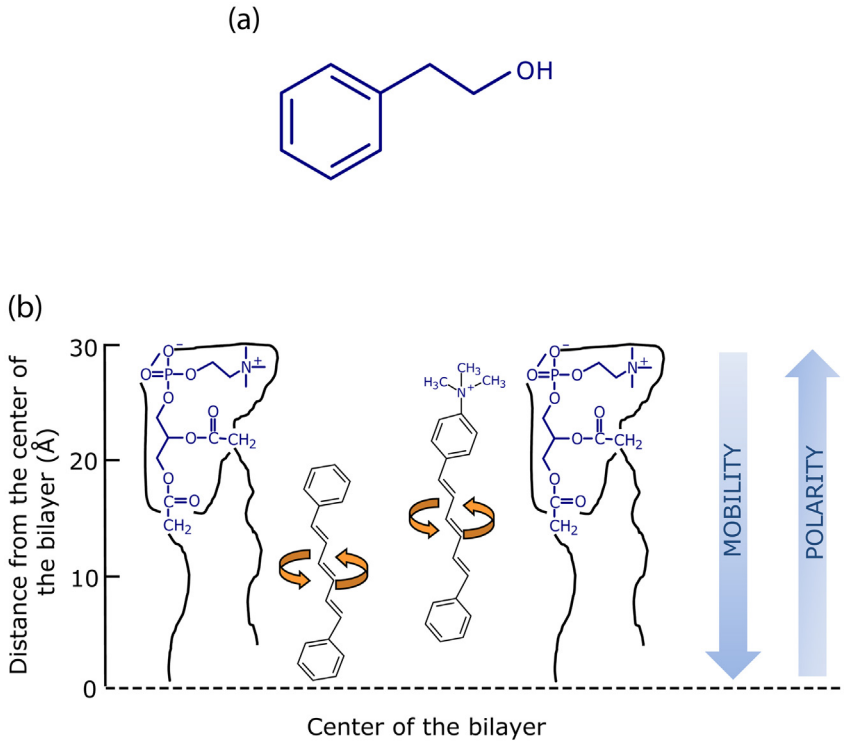

Fig. 1. (a) The chemical structure of PEtOH. (b) A schematic representation of a leaflet of the membrane bilayer showing the chemical structures and locations of the fluorescent probes DPH and TMA-DPH. The membrane location of the DPH group in these compounds are shown according to Kaiser and London (1998). The mobility and polarity gradients along the bilayer normal are also shown (see text for more details). The horizontal line at the bottom indicates the center of the bilayer.

the average depth of DPH alone has been shown to be ~8 Å from the bilayer center (Kaiser and London, 1998).

Keeping in mind the relevance of membrane phase in physical properties of membranes (van Meer et al., 2008), we explored the effect of PEtOH on the organization of membranes of varying phase. Our results show that PEtOH induces membrane fluidization (acyl chain disordering) in each of the three different membrane phases as shown by the reduction in apparent rotational correlation time of DPH and TMA-DPH with increasing concentration of PEtOH. In addition, our results suggest that local anesthetics such as PEtOH modulates membrane physical properties to the extent of even being able to induce phase separation in gel (ordered) phase membranes.

2. Materials and methods

2.1. Materials

Cholesterol, DMPC and PEtOH were purchased from Sigma Chemical Co. (St. Louis, MO). DPPC and POPC were obtained from Avanti Polar Lipids (Alabaster, AL). DPH and TMA-DPH were from Molecular Probes/Invitrogen (Eugene, OR). Phospholipids were checked for purity by thin layer chromatography on silica gel precoated plates (Sigma) in chloroform/methanol/water (65:35:5, v/v/v) and were found to provide single spot for all lipids with a phosphate-sensitive spray followed by charring (Baron and Coburn, 1984). Concentration of phospholipids were estimated by phosphate assay subsequent to complete oxidation by perchloric acid (McClare, 1971). DMPC was used as an internal standard to evaluate lipid digestion. The concentrations of stock solutions of DPH and TMA-DPH in methanol were estimated from their molar extinction coefficient (ε) of 88,000 M^{-1} cm^{-1} at 350 nm (Arora et al., 2004). All other chemicals used were of the highest purity available. Solvents used were of spectroscopic grade. Water was purified through a Millipore (Bedford, MA) Milli-Q system and used throughout.

2.2. Sample preparation

All experiments were performed using large unilamellar vesicles (LUVs) of 100 nm diameter of POPC, DPPC, or DPPC/40 mol% cholesterol with increasing concentration of PEtOH and 1 mol% probe (DPH or TMA-DPH). In general, 320 nmol of total lipid and 3.2 nmol of DPH (or TMA-DPH) were mixed well and dried under a stream of nitrogen while being warmed gently (~35 °C). After further drying under a high vacuum for at least 3 h, samples were hydrated (swelled) by addition of 1 ml of buffer (10 mM sodium phosphate, 150 mM sodium chloride, pH 7.4) containing increasing amount of PEtOH (0–2%, v/v). Each sample was vortexed for 3 min to uniformly disperse the lipids and form homogeneous multilamellar vesicles. The buffer was always maintained at a temperature well above the phase transition temperature of the phospholipid used as the vesicles were made. For this reason, lipids were swelled at a temperature of ~40 °C for POPC and ~60 °C for DPPC or DPPC/cholesterol samples. LUVs of 100 nm diameter were prepared by the extrusion technique using an Avestin Liposofast Extruder (Ottawa, Ontario, Canada) as previously described (MacDonald et al., 1991; Mukherjee and Chattopadhyay, 2005). Briefly, the multilamellar vesicles were freeze-thawed five times using liquid nitrogen to ensure solute equilibration between trapped and bulk solutions and then extruded through polycarbonate filters (pore diameter of 100 nm) mounted in an extruder fitted with Hamilton syringes (Hamilton Company, Reno, NV). The samples were subjected to 11 passes through the polycarbonate filters to give the final LUV suspension. Background samples were prepared in the same way except that DPH (or TMA-DPH) was not added to them. The optical density of the samples measured at 358 nm was less than 0.15 in all cases, which rules out any

possibility of inner filter effect or scattering artifacts. Samples were incubated in dark for 12 h at room temperature (~23 °C) for equilibration prior to fluorescence measurements. All experiments were performed with at least three sets of samples at room temperature (~23 °C).

2.3. Steady state fluorescence measurements

Steady state fluorescence anisotropy measurements were performed with a Hitachi F-7000 spectrofluorometer (Tokyo, Japan) using a Hitachi Glan-Thompson polarization accessory. Quartz cuvettes with a path length of 1 cm were used. For monitoring DPH (or TMA-DPH) fluorescence, the excitation wavelength was set at 358 nm and emission was monitored at 430 nm. Excitation and emission slits with bandpass of 1 and 5 nm were used for all measurements. The excitation slit used was the minimum possible to minimize any photoisomerization of DPH during irradiation. Fluorescence was measured with a 30 s interval between successive openings of the excitation shutter to reverse any photoisomerization of DPH (Chattopadhyay and London, 1984). Anisotropy values were calculated from the equation (Lakowicz, 2006):

$$r = \frac{I_{VV} - GI_{VH}}{I_{VV} + 2GI_{VH}} \quad (1)$$

where I_{VV} and I_{VH} are the fluorescence intensities (after appropriate background subtraction) measured with the excitation polarizer oriented vertically and the emission polarizer vertically and horizontally oriented, respectively. G is the grating factor and is the ratio of the efficiencies of the detection system for vertically and horizontally polarized light, and is equal to I_{HV}/I_{HH}.

2.4. Time-resolved fluorescence measurements

Fluorescence lifetimes were calculated from time-resolved fluorescence intensity decays using IBH 5000F NanoLED equipment (Horiba Jobin Yvon, Edison, NJ) with DataStation software in the time-correlated single photon counting (TCSPC) mode. A pulsed light-emitting diode (LED) (NanoLED-16) was used as an excitation source. This LED generates optical pulse at 337 nm with pulse duration 1.2 ns and is run at 1 MHz repetition rate. The LED profile (instrument response function) was measured at the excitation wavelength using Ludox (colloidal silica) as scatterer. To optimize the signal-to-noise ratio, 10,000 photon counts were collected in the peak channel. All experiments were performed using emission slits with bandpass of 8 nm. The sample and the scatterer were alternated after every 10% acquisition to ensure compensation for shape and timing drifts occurring during the period of data collection. This arrangement also prevents any prolonged exposure of the sample to the excitation beam, thereby avoiding any possible photodamage of the fluorophore. Data were stored and analyzed using DAS 6.2 software (Horiba Jobin Yvon, Edison, NJ). Fluorescence intensity decay curves were deconvoluted with the instrument response function and analyzed as a sum of exponential terms:

$$F(t) = \Sigma_i \alpha_i \exp(-t/\tau_i) \quad (2)$$

where F(t) is the fluorescence intensity at time t and α_i is a pre-exponential factor representing the fractional contribution to the time-resolved decay of the component with a lifetime of τ_i such that $\Sigma_i \alpha_i = 1$. The decay parameters were recovered using a nonlinear least squares iterative fitting procedure based on the Marquardt algorithm (Bevington, 1969). The program also includes statistical and plotting subroutine packages (O'Connor and Phillips, 1984). The goodness of fit of a given set of data and the chosen function was evaluated by the χ^2 ratio, the weighted residuals (Lampert et al., 1983), and the autocorrelation function of the weighted residuals (Grinvald and Steinberg, 1974). A fit was considered acceptable when plots of the weighted residuals and the autocorrelation function showed random deviation about zero with a minimum χ^2 value not more than 1.5. Intensity-averaged mean lifetimes $\langle \tau \rangle$ for biexponential decays of fluorescence were calculated from the decay times and pre-exponential factors using

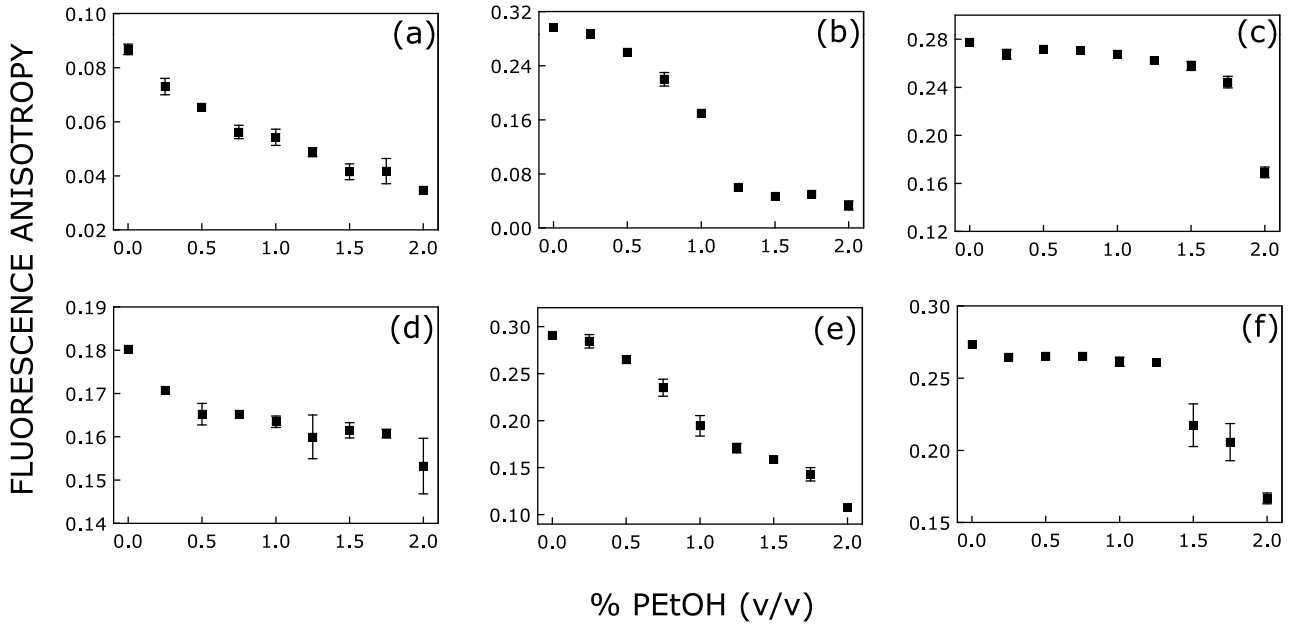

Fig. 2. Change in fluorescence anisotropy of DPH in membranes of varying phase ((a) POPC, (b) DPPC, and (c) DPPC/cholesterol) as a function of increasing concentration of PEtOH. Panels (d), (e) and (f) show fluorescence anisotropy of TMA-DPH in POPC, DPPC and DPPC/cholesterol membranes, respectively, with increasing concentrations of PEtOH. The ratio of fluorophore (DPH or TMA-DPH) to total lipid was 1:100 (mol/mol) and the total lipid concentration was 0.32 mM in all cases. The excitation wavelength was 358 nm, and emission was monitored at 430 nm. Measurements were carried out at room temperature (~23 °C). Data points shown are the means ± S.E. of at least three independent measurements. See Section 2 for other details.

Table 1
Fluorescence lifetimes of DPH with increasing PEtOH concentration.[a]

% PEtOH (v/v)	α_1	τ_1 (ns)	α_2	τ_2 (ns)
		POPC		
0	0.18	1.90	0.82	8.76
0.25	0.20	0.80	0.80	8.82
0.50	0.22	0.78	0.78	8.89
0.75	0.23	0.77	0.77	8.95
1.00	0.27	0.73	0.73	8.89
1.25	0.28	0.72	0.72	8.78
1.50	0.29	0.71	0.71	8.70
1.75	0.37	0.63	0.63	8.96
2.00	0.30	0.70	0.70	8.67
		DPPC		
0	0.62	0.22	0.38	11.04
0.25	0.85	0.13	0.15	11.14
0.50	0.80	0.11	0.20	11.25
0.75	0.87	0.15	0.13	11.29
1.00	0.79	0.15	0.21	10.80
1.25	0.87	0.12	0.13	10.88
1.50	0.92	0.12	0.08	10.45
1.75	0.95	0.11	0.05	10.50
2.00	0.95	0.11	0.05	10.66
		DPPC/Cholesterol		
0	0.78	0.01	0.22	10.69
0.25	0.85	0.08	0.15	10.69
0.50	0.78	0.02	0.22	10.69
0.75	0.89	0.08	0.11	10.65
1.00	0.93	0.06	0.07	10.71
1.25	0.84	0.10	0.16	10.80
1.50	0.85	0.09	0.15	10.82
1.75	0.99	0.01	0.01	10.69
2.00	0.96	0.04	0.04	10.76

[a] The excitation wavelength was 337 nm and emission was monitored at 430 nm. The number of photons collected at the peak channel was 10,000. All other conditions are as in Fig. 2. See Section 2 for other details.

the equation (Lakowicz, 2006):

$$\left\langle \tau \right\rangle = \frac{\alpha_1 {\tau_1}^2 + \alpha_2 {\tau_2}^2}{\alpha_1 \tau_1 + \alpha_2 \tau_2} \quad (3)$$

3. Results and discussion

3.1. Fluorescence anisotropy of DPH and TMA-DPH in membranes of varying phase with increasing concentration of PEtOH

As mentioned above, we monitored the effect of PEtOH on the organization and dynamics in membranes of varying phase. Membrane phase is an important determinant of membrane physical properties (van Meer et al., 2008). While the lipid acyl chains are ordered and extended in all *trans* conformation in the gel (ordered) phase, they are fluid and disordered (due to the *gauche* conformations of the lipid acyl chains) in the liquid-disordered (fluid) phase. The liquid-ordered phase, on the other hand, represents a phase characterized by acyl chains that are extended and ordered (such as in the gel phase), but display high lateral mobility similar to the liquid-disordered phase (Mouritsen, 2010). The liquid-ordered phase exists above a threshold level of cholesterol for binary lipid mixtures (Mouritsen, 2010). In this work, we used LUVs made of POPC, DPPC and DPPC with 40 mol% cholesterol, as these vesicles represent liquid-disordered (fluid), gel (ordered), and liquid-ordered phase membranes, respectively (Brown and London, 1998). We therefore monitored fluorescence anisotropy and lifetime of depth-dependent membrane fluorescent probes DPH and TMA-DPH in LUVs made of POPC, DPPC and DPPC/cholesterol.

The change in steady state fluorescence anisotropy of DPH and TMA-DPH in membranes of varying phase with increasing PEtOH concentration is shown in Fig. 2. Fluorescence anisotropy of membrane embedded probes, such as DPH and TMA-DPH, is related to the rotational mobility of the fluorophore in the membrane environment (Lakowicz, 2006) and is sensitive to the packing of the lipid fatty acyl chains. Fig. 2(a–c) shows decrease in fluorescence anisotropy of DPH with increasing concentration of PEtOH (0–2%, v/v) in POPC (fluid), DPPC (gel) and DPPC/cholesterol (liquid-ordered) membranes, respectively. As apparent from the figure, the anisotropy is lowest in the liquid-disordered phase (POPC). This is due to the relatively loose packing in the liquid-disordered phase. Interestingly, DPH anisotropy in the liquid-ordered (DPPC/cholesterol) phase, is much higher than that in liquid-disordered phase and appears to be comparable to the corresponding value in the gel (DPPC) phase, consistent with similar packing of lipid acyl chains in these two phases. Fig. 2(a–c) shows that DPH anisotropy exhibits a reduction in all phases although to varying extents. The maximum reduction (~89%) in anisotropy was observed in gel phase DPPC membranes with maximum concentration of PEtOH. The reduction in anisotropy at higher PEtOH concentrations (>1%, v/v) was adequate to induce phase change. This could be attributed to the fluidizing effect of PEtOH on compactly organized (tight lipid acyl chain packing) DPPC membranes in the gel phase. The reduction in anisotropy was relatively modest (~60%) in the liquid-disordered phase (POPC) with increasing concentration of PEtOH. This could be due to the relatively loose packing of the acyl chains in the liquid-disordered phase membranes. Interestingly, in case of liquid-ordered membranes (DPPC/cholesterol), DPH anisotropy displayed a characteristic dependence and remained almost invariant up to 1.75% PEtOH, followed by a sharp reduction, with an overall reduction in anisotropy of ~39%.

Table 2
Fluorescence lifetimes of TMADPH with increasing PEtOH concentration.[a]

% PEtOH (v/v)	α_1	τ_1 (ns)	α_2	τ_2 (ns)
		POPC		
0	0.37	1.13	0.63	4.40
0.25	0.35	1.04	0.65	4.05
0.50	0.33	0.99	0.67	3.78
0.75	0.33	0.95	0.67	3.50
1.00	0.33	0.94	0.67	3.40
1.25	0.33	0.89	0.67	3.20
1.50	0.34	1.00	0.66	3.06
1.75	0.31	0.90	0.69	2.90
2.00	0.41	0.96	2.59	2.40
		DPPC		
0	0.29	1.25	0.71	7.73
0.25	0.34	1.75	0.66	7.43
0.50	0.41	1.56	0.59	6.80
0.75	0.62	1.01	0.38	5.97
1.00	0.72	1.47	0.28	6.20
1.25	0.79	1.78	0.21	6.01
1.50	0.81	1.86	0.19	5.41
1.75	0.52	1.40	0.48	3.24
2.00	0.42	1.04	0.58	2.54
		DPPC/cholesterol		
0	0.10	1.81	0.90	9.01
0.25	0.09	2.02	0.91	8.95
0.50	0.09	1.62	0.91	8.87
0.75	0.11	1.16	0.89	8.96
1.00	0.13	1.94	0.87	8.86
1.25	0.12	1.64	0.88	8.87
1.50	0.59	2.50	0.41	8.05
1.75	0.67	2.40	0.33	7.80
2.00	0.68	1.81	0.32	4.16

[a] The excitation wavelength was 337 nm and emission was monitored at 430 nm in all cases. The number of photons collected at the peak channel was 10,000. All other conditions are as in Fig. 2. See Section 2 for other details.

As mentioned above, in order to comprehensively monitor membrane order in membranes of varying phase due to PEtOH, we monitored the change in membrane order at a shallow location in the membrane using TMA-DPH, in which the DPH moiety is localized at the membrane interface (Kaiser and London, 1998). Fig. 2d shows that fluorescence anisotropy was higher in case of TMA-DPH compared to DPH in POPC (fluid) membranes. This is indicative of shallow membrane localization of the DPH group in TMA-DPH, keeping in mind the mobility gradient along the bilayer normal in fluid phase membranes (Haldar et al., 2011). Fig. 2(d–f) shows the change in fluorescence anisotropy of TMA-DPH in varying phase membranes with increasing concentration of PEtOH. The figure shows that the anisotropy of TMA-DPH is reduced in all cases. The extent of anisotropy change was most (~63%) in gel phase (DPPC), similar to what was observed with DPH (see Fig. 2b). However, the extent of anisotropy change was lowest (~15%) in fluid phase (POPC) when TMA-DPH was used as a fluorophore, much lower than the corresponding reduction in anisotropy observed with DPH. This could be due to relatively shallow localization of the DPH group in TMA-DPH in the membrane. Anisotropy change was similar (~39%) in case of liquid-ordered phase membranes. Taken together, these results suggest that the changes induced by PEtOH in varying phase membranes affect the organization of the membrane bilayer and these effects are not uniform along the membrane normal.

3.2. Fluorescence lifetime of DPH and TMA-DPH in varying phase membranes: effect of PEtOH

Fluorescence lifetime provides information about immediate vicinity of a fluorophore in which it is placed (Prendergast, 1991). In particular, the fluorescence lifetime of DPH is sensitive to the polarity changes in its surroundings (Stubbs et al., 1995; Shrivastava et al., 2008). The lifetimes of DPH and TMA-DPH in membranes of varying phase are shown in Tables 1 and 2. All fluorescence decays could be fitted well to a biexponential function. We calculated the intensity-averaged mean fluorescence lifetime since it is independent of the method of analysis and the number of exponentials used to fit the time-resolved fluorescence decay. The mean fluorescence lifetimes of DPH and TMA-DPH in membranes of varying phase were calculated from data shown in Tables 1 and 2 using Eq. (3), and are shown in Fig. 3. The mean fluorescence lifetime of DPH was more compared to TMA-DPH in all phases, thereby indicating more polar environment around TMA-DPH, possibly due to differential water penetration in these two cases (Stubbs et al., 1995). The mean fluorescence lifetime of DPH was found to be maximum (~10.7 ns) in gel phase (DPPC) and liquid-ordered phase (DPPC/cholesterol) membranes, due to tighter packing of acyl chains in both cases (thereby minimizing water penetration). The mean fluorescence lifetimes of DPH in liquid-disordered phase (POPC) membranes was found to be shorter (~8.7 ns), indicating relatively polar environment around DPH attributed to loose packing of acyl chains in the fluid phase. The corresponding changes in mean fluorescence lifetime of TMA-DPH are shown in Fig. 3(d–f). Fig. 3(a–c) shows progressive reduction in the mean fluorescence lifetime of DPH in membranes of varying phase with increasing PEtOH concentration. This could indicate a gradual change in membrane polarity around the DPH moiety with increasing PEtOH concentration, perhaps due to the disordering induced by PEtOH, thereby increasing water penetration in the membrane. Similar results were observed with TMA-DPH in varying phase membranes with increasing PEtOH concentration and are shown in Fig. 3(d–f).

3.3. Apparent rotational correlation time of DPH and TMA-DPH in membranes of varying phase in presence of PEtOH

To ensure that the fluorescence anisotropy values measured for DPH or TMA-DPH (Fig. 2) are not affected by fluorescence lifetime-induced artifacts, we calculated the apparent rotational correlation times using Perrin's equation (Lakowicz, 2006):

$$\tau_c = \frac{\langle\tau\rangle r}{r_o - r} \quad (4)$$

where r_o is the fundamental anisotropy (i.e., in the absence of depolarizing processes such as rotational diffusion), r is the steady

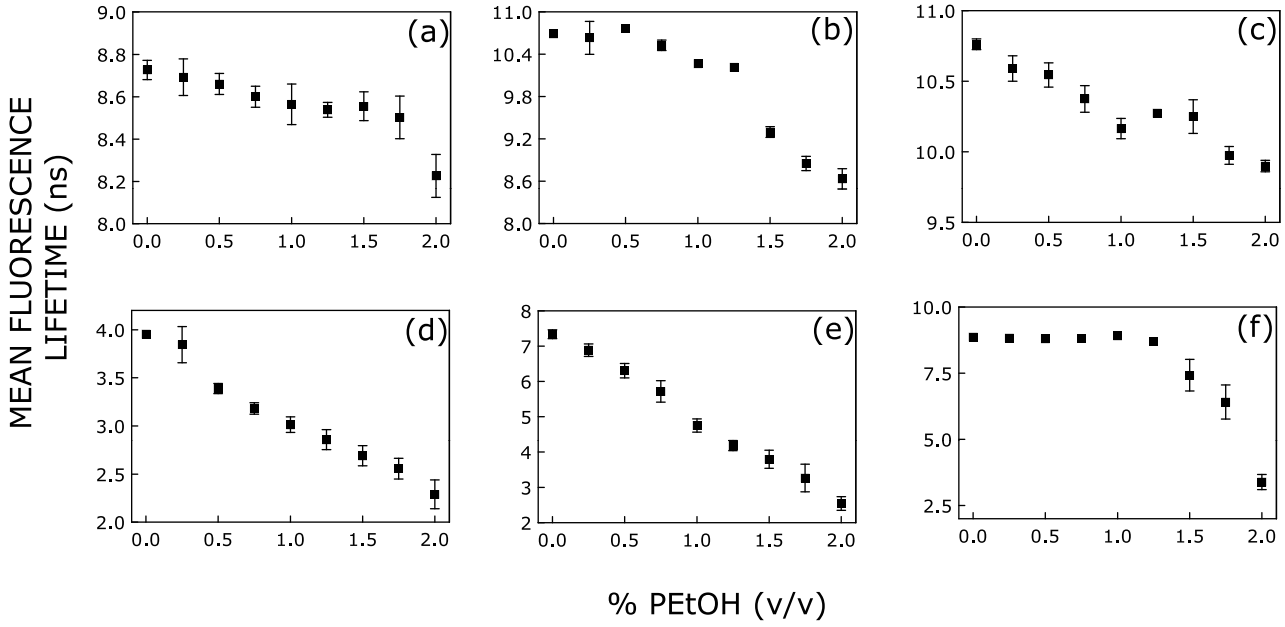

Fig. 3. Effect of increasing concentration of PEtOH on mean fluorescence lifetime of DPH in (a) POPC, (b) DPPC and (c) DPPC/cholesterol membranes. Panels (d–f) show change in mean fluorescence lifetime of TMA-DPH in POPC, DPPC and DPPC/cholesterol membranes with increasing concentration of PEtOH. Mean fluorescence lifetimes were calculated using Eq. (3). The excitation wavelength was 337 nm and emission was monitored at 430 nm in all cases. All other conditions are as in Fig. 2. See Section 2, and Tables 1 and 2 for more details.

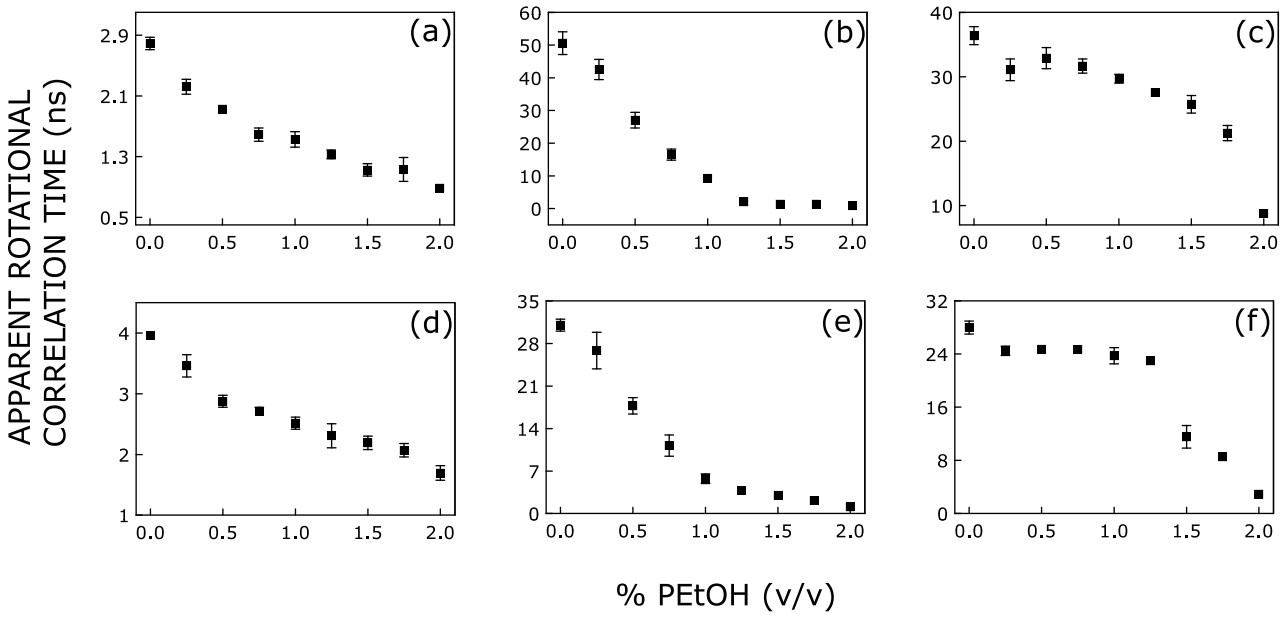

Fig. 4. Apparent rotational correlation times of DPH (a-c) and TMA-DPH (d-f) in POPC, DPPC and DPPC/cholesterol membranes, with increasing PEtOH concentration. Apparent rotational correlation times were calculated from fluorescence anisotropy values from Fig. 2 and mean fluorescence lifetimes from Fig. 3 using Eq. (4). See text for other details.

state fluorescence anisotropy (from Fig. 2), and $\langle\tau\rangle$ is the mean fluorescence lifetime (from Fig. 3). While Perrin's equation is not strictly valid in this case, we treat this as an approximation, particularly because we used mean fluorescence lifetimes for the analysis of multiple component lifetimes. The apparent rotational correlation times, calculated this way using a value of r_o of 0.36 (Shinitzky and Barenholz, 1974), are shown in Fig. 4. Both in case of DPH and TMA-DPH, the apparent rotational correlation time was found to be highest (~50.6 and 31.0 ns) in gel phase (DPPC) membranes, indicative of the motional restriction experienced by the probe in the gel phase. The apparent rotational correlation time was found to be least (~2.8 and 4.0 ns) in fluid phase (POPC) membranes. The calculated values for apparent rotational correlation time in the liquid-ordered phase (DPPC/cholesterol) membranes were intermediate (~36.4 and 28.0 ns). The change in apparent rotational correlation times with increasing concentration of PEtOH exhibited similar trends (see Fig. 2 for changes in anisotropy), which indicates that the fluorescence anisotropy values are free from fluorescence lifetime-induced artifacts.

The overall goal of this work is to explore the effect of the local anesthetic PEtOH on organization and dynamics in membranes representing various biologically relevant phases. It was earlier reported that PEtOH could fluidize model and *E. coli* membranes using generalized polarization of the fluorescent probe laurdan and NMR (Anbazhagan et al., 2010; Jordi et al., 1990; Killian et al., 1992). However, information about localized fluidity changes and effect of membrane phase on such change was lacking. As previously mentioned, monitoring site-specific dynamic change in membranes provides comprehensive information since the dynamic change could vary depending on the location in the membrane. Toward this goal, we have utilized two fluorescent membrane probes DPH and TMA-DPH, as they provide information on rotational dynamics from different depths in the membrane. In addition, keeping in mind the crucial role of membrane phase, we have monitored changes in lipid acyl chain packing using differentially localized fluorescent probes in three phases which are relevant in biology. Our results show that PEtOH induces membrane disorder in membranes of all three phases, although the extent of disordering varies in a phase-dependent manner. For example, the maximum disordering by PEtOH was observed in gel phase membranes, followed by liquid-ordered membranes. The disordering was least in fluid phase membranes. The disordering effect of PEtOH in gel phase membranes is large enough to induce concentration-dependent phase change, as apparent from the fluorescence anisotropy of DPH in gel phase DPPC membranes at PEtOH concentrations >1% (v/v) (see Fig. 2b). Our results could assume significance in natural membranes where ordered and disordered membranes could co-exist (Saxena et al., 2015), and could be relevant in the context of the role of anesthetics in membrane protein function.

Conflict of interest

The authors declare that there is no conflict of interest.

Acknowledgments

This work was supported by the Council of Scientific and Industrial Research, Govt. of India. A.C. is an Adjunct Professor of Tata Institute of Fundamental Research (Mumbai), RMIT university (Melbourne, Australia), Indian Institute of Technology (Kanpur), and Indian Institute of Science Education and Research (Mohali). A. C. gratefully acknowledges J.C. Bose Fellowship (Department of Science and Technology, Govt. of India). We thank members of the Chattopadhyay laboratory for their comments and discussions.

References

Anbazhagan, V., Munz, C., Tome, L., Schneider, D., 2010. Fluidizing the membrane by a local anesthetic: phenylethanol affects membrane protein oligomerization. J. Mol. Biol. 404, 773–777.
Arias, H.R., 1999. Role of local anesthetics on both cholinergic and serotonergic ionotropic receptors. Neurosci. Biobehav. Rev. 23, 817–843.
Arora, A., Raghuraman, H., Chattopadhyay, A., 2004. Influence of cholesterol and ergosterol on membrane dynamics: a fluorescence approach. Biochem. Biophys. Res. Commun. 318, 920–926.
Baron, C.B., Coburn, R.F., 1984. Comparison of two copper reagents for detection of saturated and unsaturated neutral lipids by charring densitometry. J. Liq. Chromatogr. 7, 2793–2801.

Bevington, P.R., 1969. Data Reduction and Error Analysis for the Physical Sciences. McGraw-Hill, New York.
Brown, D.A., London, E., 1998. Structure and origin of ordered lipid domains in biological membranes. J. Membr. Biol. 164, 103–114.
Chattopadhyay, A., London, E., 1984. Fluorimetric determination of critical micelle concentration avoiding interference from detergent charge. Anal. Biochem. 139, 408–412.
Gray, E., Karslake, J., Machta, B.B., Veatch, S.L., 2013. Liquid general anesthetics lower critical temperatures in plasma membrane vesicles. Biophys. J. 105, 2751–2759.
Grinvald, A., Steinberg, I.Z., 1974. On the analysis of fluorescence decay kinetics by the method of least-squares. Anal. Biochem. 59, 583–598.
Haldar, S., Chaudhuri, A., Chattopadhyay, A., 2011. Organization and dynamics of membrane probes and proteins utilizing the red edge excitation shift. J. Phys. Chem. B 115, 5693–5706.
Jordi, W., Nibbeling, R., de Kruijff, B., 1990. Phenethyl alcohol disorders phospholipid acyl chains and promotes translocation of the mitochondrial precursor protein apocytochrome *c* across a lipid bilayer. FEBS Lett. 261, 55–58.
Kaiser, R.D., London, E., 1998. Location of diphenylhexatriene (DPH) and its derivatives within membranes: comparison of different fluorescence quenching analyses of membrane depth. Biochemistry 37, 8180–8190.
Killian, J.A., Fabrie, C.H.J.P., Baart, W., Morein, S., de Kruijff, B., 1992. Effects of temperature variation and phenethyl alcohol addition on acyl chain order and lipid organization in *Escherichia coli* derived membrane systems A ^{2}H- and ^{31}P-NMR study. Biochim. Biophys. Acta 1105, 253–262.
Kitagawa, S., Hirata, H., 1992. Effects of alcohols on fluorescence anisotropies of diphenylhexatriene and its derivatives in bovine blood platelets: relationships of the depth-dependent change in membrane fluidity by alcohols with their effects on platelet aggregation and adenylate cyclase activity. Biochim. Biophys. Acta 1112, 14–18.
Lakowicz, J.R., 2006. Principles of Fluorescence Spectroscopy, 3rd ed. Springer, New York.
Lampert, R.A., Chewter, L.A., Phillips, D., O'Connor, D.V., Roberts, A.J., Meech, S.R., 1983. Standards for nanosecond fluorescence decay time measurements. Anal. Chem. 55, 68–73.
MacDonald, R.C., MacDonald, R.I., Menco, B.P., Takeshita, K., Subbarao, N.K., Hu, L.-R., 1991. Small-volume extrusion apparatus for preparation of large, unilamellar vesicles. Biochim. Biophys. Acta 1061, 297–303.
McClare, C.W.F., 1971. An accurate and convenient organic phosphorus assay. Anal. Biochem. 39, 527–530.
Mouritsen, O.G., 2010. The liquid-ordered state comes of age. Biochim. Biophys. Acta 1798, 1286–1288.
Mukherjee, S., Chattopadhyay, A., 2005. Influence of ester and ether linkage in phospholipids on the environment and dynamics of the membrane interface: a wavelength-selective fluorescence approach. Langmuir 21, 287–293.
O'Connor, D.V., Phillips, D., 1984. Time-correlated Single Photon Counting. Academic Press, London, pp. 180–189.
Prendergast, F.G., Haugland, R.P., Callahan, P.J., 1981. 1-[4-(Trimethylamino)phenyl]-6-phenylhexa-1,3,5-triene: synthesis, fluorescence properties and use as a fluorescence probe of lipid bilayers. Biochemistry 20, 7333–7338.
Prendergast, F.G., 1991. Time-resolved fluorescence techniques: methods and applications in biology. Curr. Opin. Struct. Biol. 1, 1054–1059.
Rehberg, B., Urban, B.W., Duch, D.S., 1995. The membrane lipid cholesterol modulates anesthetic actions on a human brain ion channel. Anesthesiology 82, 749–758.
Revathi, C.J., Chattopadhyay, A., Srinivas, U.K., 1994. Change in membrane organization induced by heat shock. Biochem. Mol. Biol. Int. 32, 941–950.
Saxena, R., Shrivastava, S., Chattopadhyay, A., 2015. Cholesterol-induced changes in hippocampal membranes utilizing a phase-sensitive fluorescence probe. Biochim. Biophys. Acta 1848, 1699–1705.
Shinitzky, M., Barenholz, Y., 1974. Dynamics of the hydrocarbon layer in liposomes of lecithin and sphingomyelin containing dicetylphosphate. J. Biol. Chem. 249, 2652–2657.
Shrivastava, S., Paila, Y.D., Dutta, A., Chattopadhyay, A., 2008. Differential effects of cholesterol and its immediate biosynthetic precursors on membrane organization. Biochemistry 47, 5668–5677.
Stubbs, C.D., Ho, C., Slater, S.J., 1995. Fluorescence techniques for probing water penetration into lipid bilayers. J. Fluoresc. 5, 19–28.
Tieman, D., Taylor, M., Schauer, N., Fernie, A.R., Hanson, A.D., Klee, H.J., 2006. Tomato aromatic amino acid decarboxylases participate in synthesis of the flavor volatiles 2-phenylethanol and 2-phenylacetaldehyde. Proc. Natl. Acad. Sci. U. S. A. 103, 8287–8292.
van Meer, G., Voelker, D.R., Feigenson, G.W., 2008. Membrane lipids: where they are and how they behave. Nat. Rev. Mol. Cell Biol. 9, 112–124.